Mon. Not. R. Astron. Soc. **000**, 000–000 (0000) Printed 1 February 2008 (MN LATEX style file v1.4)

Pulsar Timing at Urumqi Astronomical Observatory: Observing System and Results

N. Wang,[1,2,3⋆] R. N. Manchester,[2] J. Zhang,[1] X. J. Wu,[3]
A. Yusup,[1] A. G. Lyne,[4] K. S. Cheng[5] and M. Z. Chen[1]

[1] *Urumqi Astronomical Observatory, NAO-CAS, 40 South Beijing Road, Urumqi, 830011, China*
[2] *Australia Telescope National Facility, CSIRO, PO Box 76, Epping, NSW 1710, Australia*
[3] *Astronomy Department, Peking University, Beijing, 100871, China*
[4] *University of Manchester, Jodrell Bank Observatory, Macclesfield, Cheshire SK11 9DL*
[5] *Physics Department, Hong Kong University*

1 February 2008

ABSTRACT

A pulsar timing system has been operating in the 18-cm band at the Urumqi Astronomical Observatory 25-m telescope since mid-1999. Frequency resolution allowing dedispersion of the pulsar signals is provided by a $2\times128\times2.5$ MHz filterbank/digitiser system. Observations of 74 pulsars over more than 12 months have resulted in updated pulsar periods and period derivatives, as well as improved positions. Comparison with previous measurements showed that the changes in period and period derivative tend to have the same sign and to be correlated in amplitude. A model based on unseen glitches gives a good explanation of the observed changes, suggesting that long-term fluctuations in period and period derivatives are dominated by glitches. In 2000 July, we detected a glitch of relative amplitude $\Delta\nu/\nu \sim 24\times10^{-9}$ in the Crab pulsar. The post-glitch decay appears similar to other large Crab glitches.

Key words: pulsars:general

1 INTRODUCTION

Pulsars are remarkable celestial clocks. They act as probes for many different studies, including investigations of the interstellar medium, stellar and binary system evolution, relativistic astrophysics and condensed matter. Identified as rotating neutron stars, they have an observed pulse period range of 0.0016 to 8.5 s. Because of the huge moment of inertia ($\sim 10^{45}$ g cm^2) and compact nature of a neutron star, the rotation periods are very stable. However, they are not completely constant, increasing gradually as the pulsar loses energy in the form of relativistic particles and electromagnetic radiation with small variations due to changes in the stellar structure. Pulse timing observations can be used to accurately measure the pulse periods and these variations, including effects related to the orbital motion for binary pulsars, precise positions and proper motions and even annual parallax for some pulsars.

If we express the pulsar rotation frequency as a Taylor series, the pulse phase at time t is given by

$$\phi(t) = \phi_0 + \nu t + \frac{1}{2}\dot{\nu}t^2 + \frac{1}{6}\ddot{\nu}t^3 + \cdots, \quad (1)$$

where the rotation frequency $\nu = 1/P$, where P is the pulse period, $\dot{\nu}$ and $\ddot{\nu}$ are the first and second time derivatives of the pulse frequency, and t is the time in a frame which is inertial with respect to the pulsar, normally taken to be the solar-system barycenter frame. The differences between observed pulse arrival times (TOAs) and those predicted from Equation 1, are known as timing residuals. Timing residuals will deviate from zero if the model is not accurate, for example, due to errors in the frequency parameters or irregularities in the pulse period. Given a set of TOAs from timing observations at different epochs t, corrections to the rotation and astrometric parameters can be obtained by performing a least-square fit to minimise the residuals. Improved positions, with an accuracy of the order 0.1 arcsec, can be obtained from TOAs spanning a year or more, because an error in position gives rise to an annual term in the timing residuals due to the orbital motion of the Earth.

Two kinds of timing irregularities are observed in pulsars. The first is timing noise, characterised by random period changes with the fractional amplitude about 10^{-9} s or less with time scales of days, months or years (Cordes & Downs 1985; Arzoumanian et al. 1994). The second kind of timing irregularity is known as a 'glitch', where the pulse frequency suddenly increases with the fractional amplitude

⋆ Email: wangna@ms.xjb.ac.cn

$\Delta\nu/\nu$ typically in the range 10^{-9} – 10^{-6} (Lyne, Shemar & Graham-Smith 2000; Wang et al. 2000). Glitches are unpredictable but typically occur at intervals of a few years in young pulsars. Coincident with the glitch, there is often an increase in the magnitude of the frequency derivative, typically by ~ 1 per cent, which sometimes has an approximately exponential decay with a time scale of weeks to years.

Because of these unpredictable changes, period parameters lose their validity with time. However, for some pulsars, parameters have not been updated for 30 years (Taylor, Manchester & Lyne 1993), and hence it is desirable to improve them. Moreover, to study the properties of timing noise and glitches, frequent timing observations are required.

The 25-m radio telescope at Nanshan, operated by Urumqi Astronomical Observatory (UAO), is ideal for such applications. It is mainly used as a VLBI station and has receivers for six wavelength bands: 1.3 cm, 3.6/13 cm, 6 cm, 18 cm and 92 cm. The telescope is available for pulsar timing for about two days every week, and so frequent observations are possible. To overcome the undesirable effects of high Galactic background emission and of propagation in the interstellar medium, especially scattering at longer wavelength, we decided to use the 18-cm band for the pulsar timing observations. A timing system based on a room-temperature receiver has been operational since mid-1999. In Section 2 of this paper, the receiver and data acquisition system are introduced. Observations and data analysis are discussed in Section 3. In Section 4, we present new measurements of positions, discuss period and period derivative changes and introduce a glitch detected in the Crab pulsar. We discuss and summarise our work in Section 5.

2 RECEIVER AND DATA ACQUISITION SYSTEM

A pulsar timing system has been established at the Nanshan Station of Urumqi Astronomical Observatory, located near the geographic center of Asia, with longitude 87° and latitude +43°. The timing system operates in the 18-cm band and is outlined in Fig. 1. For this band, the telescope has cassegrain optics and uses a horn feed receiving orthogonal circular polarisations. The receiver has dual-channel, room-temperature pre-amplifiers with center radio frequency (RF) of 1540 MHz and total bandwidth of 320 MHz. The system temperature is approximately 100 K. The polarisations are split by an ortho-mode transducer (OMT) at the end of the feed, amplified and then down-converted to intermediate frequency (IF) in the range 80–400 MHz using a local oscillator (LO) at 1300 MHz. After conversion, the signals are fed to a filterbank system which has 128 2.5-MHz channels for each polarisation.

Each of the 256 analogue signals from the filterbank pass through a 0.2 Hz high-pass filter and are then integrated and 1-bit digitised. Digitised data are grouped in blocks of 32 bits for transfer to the on-line computer. The digitiser uses 1-sec and 5-sec pulses derived from the Observatory H-maser to start the data conversion at a known time. The observation is started by the 1-sec pulse and the start time is checked using the 5-sec pulse. The sampling interval is adjustable as a multiple of 1 μs, clocked by a 1 MHz reference signal, also derived from the Observatory H-maser. The first

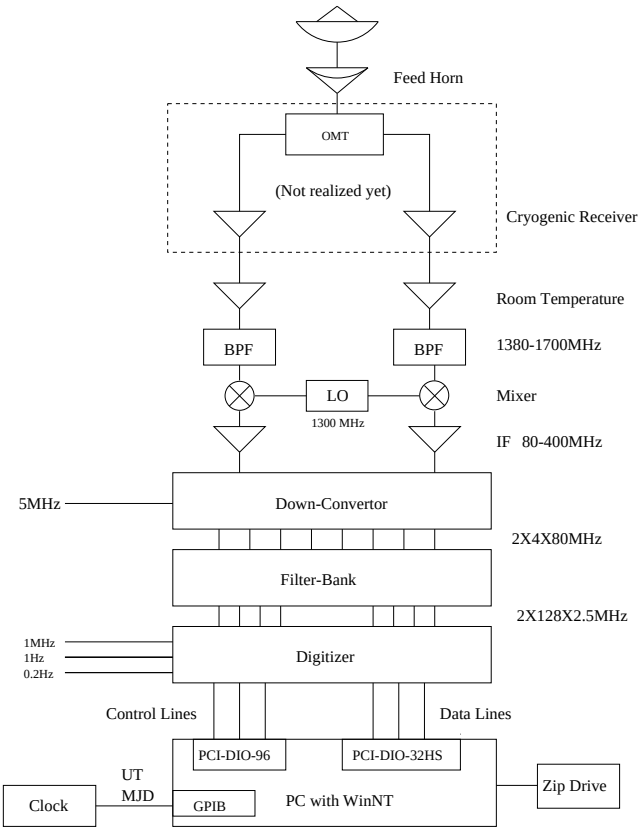

Figure 1. Diagram of the pulsar timing system at Urumqi Astronomical observatory. The center frequency is 1540 MHz and the received bandwidth and the received band is defined by bandpass filters (BPF) after the RF amplifiers. The ortho-mode transducer (OMT) and the receiver preamplifiers are currently at room temperature but will soon be replaced by a cryogenically cooled system. De-dispersion is provided by a $2 \times 128 \times 2.5$ MHz filterbank and digitiser. The digitiser is controlled by a PC computer using National Instruments interface cards.

word of each sample is a counter which is checked by the data acquisition program. A GPS time-transfer system is used to align the Observatory clock with UTC.

Signals from each channel are recorded by a data acquisition system based on a PC operating under Windows NT. The online program (Pulsar Timing Data Acquisition) is written in Visual C++. It has threads to perform several tasks at the same time, including setting the digitiser parameters and data sampling, unpacking data and checking time synchronisation, folding of channel data and saving data to disk, dedispersing and displaying of folded profiles and communicating with the computer which controls the telescope. The program reads in the date and UTC from the clock. A run-line is set high before the chosen start time and the sampling is triggered by the rising edge of the next 1-sec pulse. Unpacked data for each channel are folded at the apparent pulsar period, updated at 120-s intervals, to form sub-integrations of typical duration 240 s. Predicted topocentric periods are calculated using 'polyco' files produced by the pulsar timing program TEMPO†. Folded data

† See http://www.atnf.csiro.au/research/pulsar/timing/tempo/

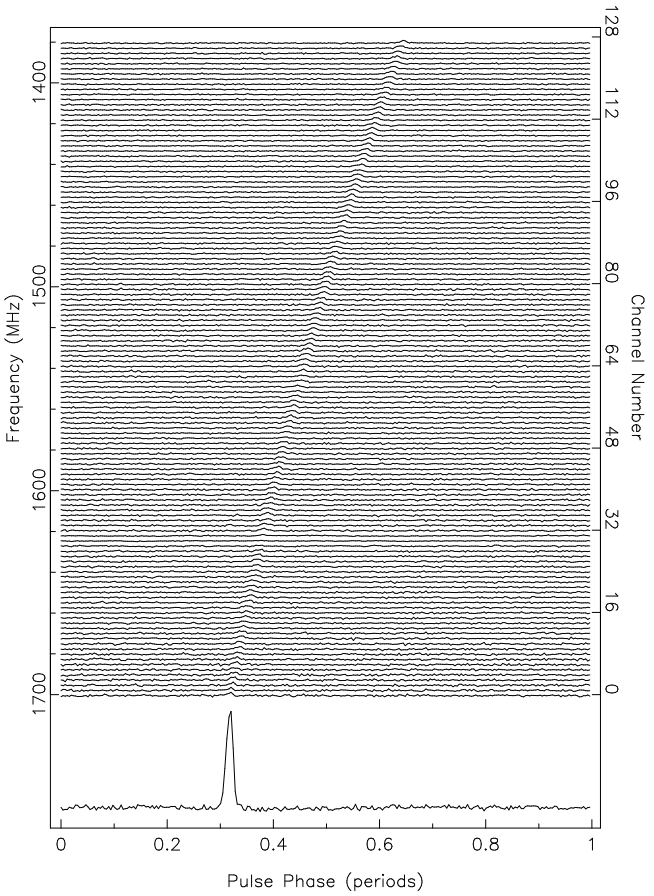

Figure 2. Pulse profiles of PSR B1933+16. The upper part shows the profile in each of the 128 2.5MHz channels, the lower part is the sum of all the channels after appropriate shifts for dispersion have been applied.

are saved to disk at every sub-integration time. The sequence counter and synchronisation flag produced by the digitiser are checked every sample and on each 5 second respectively. Folded profiles, including each channel, the sum of each polarisation and total power, are displayed for monitor purposes (See Fig. 2) and are refreshed about once per second.

3 OBSERVATIONS AND DATA ANALYSIS

The sensitivity of pulsar observations is affected by receiver, spillover and Galactic background noise ($T_{\rm rec}$, $T_{\rm spl}$ and $T_{\rm bkg}$), antenna gain (G), receiver bandwidth ($\Delta\nu$), integration time ($t_{\rm int}$), effective pulse width (W) and pulse period (P). The limiting mean flux density is given by:

$$S_{\rm min} = \frac{\alpha\beta(T_{\rm bkg}+T_{\rm spl}+T_{\rm rec})}{G\sqrt{N_{\rm p}\Delta\nu t_{\rm int}}}\sqrt{\frac{W}{P-W}}, \qquad (2)$$

where $\alpha \sim 5$ is the threshold signal-to-noise ratio for timing, $\beta \sim 1.5$ is digitisation and other processing losses, $T_{\rm bkg} + T_{\rm spl} + T_{\rm rec} \sim 100$ K, $G \sim 0.1$ K Jy^{-1}, $N_{\rm p} = 2$ is the number of polarisations and $\Delta\nu = 320$ MHz (Dewey et al. 1985). For a typical pulsar with a duty cycle $W/P \sim 0.05$, Equation 2 gives a sensitivity of $S_{\rm min} \sim 2.2$ mJy for $t_{\rm int} \sim 16$ mins.

The pulsar catalogue (Taylor, Manchester & Lyne 1993) gives flux densities, S, for most pulsars at 400 MHz and 1400 MHz. We first selected pulsars that are north of declination -40° and have $S_{1400} > S_{\rm min}$. For those where there are no 1400 MHz measurements, we assume a power law spectrum $S \propto f^\alpha$, where f is the observing frequency and $\alpha = -1.7$, to estimate S_{1400} from S_{400}. All these pulsars were observed from October 1999 to December 1999. From December, only those pulsars where significant emission was detected in 16 minutes were observed. There were 74 such pulsars and these generally had $S_{1400} > 4$ mJy. All of these pulsars are 'normal' (non-millisecond) pulsars. Their positions on a $P - \dot{P}$ diagram are shown in Fig. 3. Observations are made once or twice per week with most being of 16 minutes duration. In this paper we present observations for these 74 pulsars up to February 2001.

After each observation, the data are moved to a Linux system and compressed using the program TREDUCE (supported by Swinburne University of Technology and ATNF) to form the archive files. These archive files consist 8 subbands in each polarisation and 4 sub-integrations. The archives are first dedispersed relative to the center frequency and summed in time by TREDUCE to form one mean pulse profile per observation. TOAs are obtained using an iterative process. First a profile with good signal-to-noise ratio is adopted as a 'standard profile' or template. This template is cross-correlated with the observed mean pulse profiles to produce TOAs. TEMPO is used to reduce TOAs to arrival times at infinite frequency at the Solar system barycentre using the JPL Solar system ephemeris DE200 (Standish 1982), compute timing residuals and do a least-square fit to determine a preliminary set of improved model parameters. Using these parameters, all observed profiles are summed to produce a high signal-to-noise ratio mean pulse profile which is then adopted as a standard profile for subsequent TEMPO analyses. As examples, Fig. 4 shows six final standard profiles. For the mode-changing pulsar PSR B0329+54, two standard profiles are formed for the different modes and TOAs are obtained using the appropriate profile.

4 RESULTS

In this section we present the results of timing analyses of 74 pulsars. These results are compared with previously published data from the pulsar catalogue. In addition we checked recent publications on pulsar timing and astrometry to obtain the best periods, period derivatives and positions. We fit for position, period and period first derivative for all pulsars except as noted below. The epochs of periods and positions are fixed at MJD 51700, near the center of our data span. PSRs B1754−24 and B1800−21 lie near the ecliptic plane and so their declinations cannot be determined from timing fits. The Crab pulsar suffered a glitch during the year and is discussed separately.

4.1 Positions

Pulsar positions from the catalogue and this work are present in Table 1; superscripts 'c' and 'o' stand for catalogue value and observed value respectively. Parameter uncertainties in this and subsequent tables are given in paren-

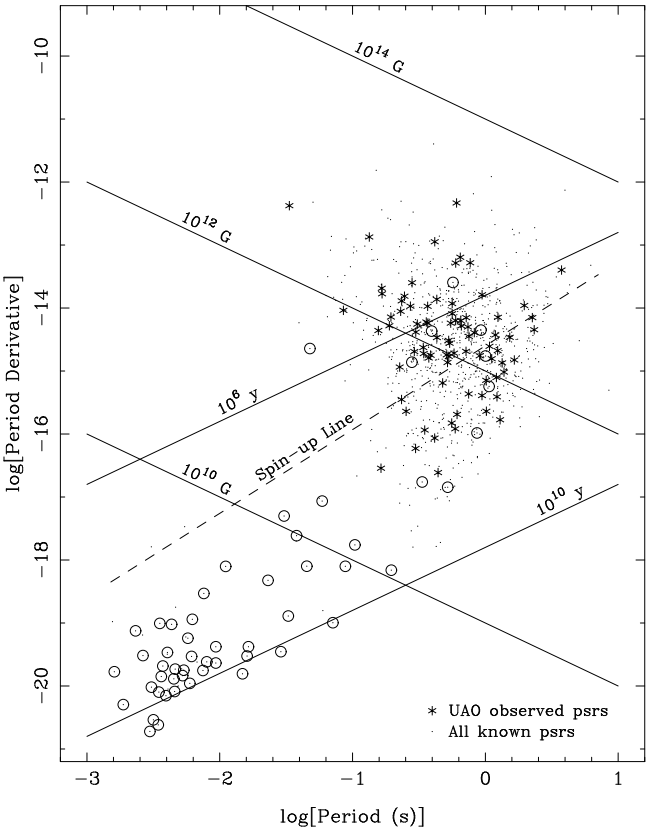

Figure 3. $P - \dot{P}$ diagram of known pulsars. Pulsars observed at UAO are marked as stars. Binary pulsars are indicated by a circle around the point and lines of constant surface dipole magnetic field and characteristic age are shown. The spin-up line for millisecond pulsars is indicated by a dashed line.

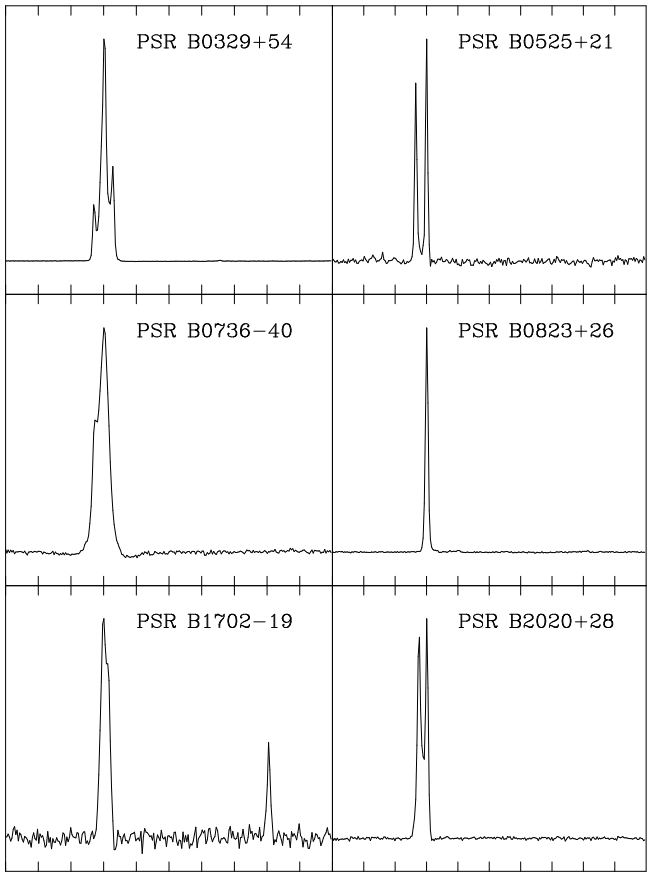

Figure 4. Examples of standard pulse profiles obtained from the observations which are used as templates to form the TOAs. The full pulse period is shown for each profile.

theses and refer to the last quoted digit. For the observed parameters, they are the 1-σ errors given by TEMPO. References for catalogue positions are given in column 5 and the data span of our observations is given in the last column.

Among these pulsars, PSR B1754−24 had a very large sinusoid timing residual before fitting for position. Since it lies close to the ecliptic plane, timing measurements cannot determine an accurate declination. The best previously published measurements are R.A.(J2000) = $17^{\rm h}57^{\rm m}40^{\rm s}(60)$ (Taylor, Manchester & Lyne 1993) and Dec.(J2000) = $-24°21'57''(30)$ (Vivekanand, Mohanty & Salter 1983). In our analysis, we fix the declination at the catalogue value and fit for R.A. along with the other timing parameters. The error of R.A. was estimated by taking the quadrature sum of the TEMPO R.A. error at the nominal declination and half of the difference in the R.A. in TEMPO fits with the declination held at each end of its uncertainty range. This gives the greatly improved value R.A.(J2000) = $17^{\rm h}57^{\rm m}29\overset{\rm s}{.}32(3)$. Similarly, for PSR B1800−21 we obtained R.A.(J2000) = $18^{\rm h}03^{\rm m}51\overset{\rm s}{.}15(3)$, significantly different from the catalogue value.

In principle, the parameters given in Table 1 can be used to estimate the pulsar proper motions and (two-dimensional) space velocities. However, with only one year of data, it is impossible to separate the effects of proper motion and long-period timing noise, leading to possible systematic errors in the derived proper motions. We therefore defer this analysis to a time when more data are available.

4.2 Period Parameters

Improved periods and period derivatives at epoch MJD 51700 are given in Table 2 for all observed pulsars except the Crab pulsar. Column 5 gives the number of TOAs and column 6 the timing residual in microseconds.

By comparing the observed and catalogue values, we obtain the period and period derivative changes, ΔP and $\Delta\dot{P}$ given in columns 7 and 8 respectively. The time interval from the epoch of the catalogue period to MJD 51700 is given in column 9. There are seven pulsars for which glitches have been detected in previous observations: PSRs B0355+54, B0525+21, B0531+21, B1508+55, B1737−30, B1800−21 and B1830−08 (Lyne, Shemar & Graham-Smith 2000; Wang et al. 2000). We quote the latest published post-glitch rotation parameters for comparison. The Crab pulsar (PSR B0531+21) glitched in July 2000; results for it are discussed in Section 4.3.

Significant differences between the observed and predicted periods are observed for most pulsars. Some pulsars, such as PSRs B0628−28, B0844−35, B1737−39, B1834−10 and B1845−01, the period changes are positive and larger than 10^{-8} s. In contrast, PSRs B1700−32, B1706−16, B1754−24 and B1822−09 have periods about

Table 1. Pulsars positions from catalogue and this work.

PSR J	PSR B	α^c(J2000) (^{h} ^{m} ^{s})	δ^c(J2000) ($^\circ$ $'$ $''$)	Ref.[a]	α^o(J2000) (^{h} ^{m} ^{s})	δ^o(J2000) ($^\circ$ $'$ $''$)	Data Span MJD
0034−0721	0031−07	00:34:08.88(3)	−07:21:53.4(7)	1	00:34:08.87(5)	−07:21:54.7(11)	51560–51948
0139+5814	0136+57	01:39:19.770(3)	+58:14:31.85(3)	2	01:39:19.740(7)	+58:14:31.94(4)	51547–51966
0141+6009	0138+59	01:41:39.947(7)	+60:09:32.28(5)	3	01:41:39.97(5)	+60:09:32.28(17)	51560–51915
0332+5434	0329+54	03:32:59.35(1)	+54:34:43.2(1)	1	03:32:59.367(7)	+54:34:43.44(9)	51499–51967
0358+5413	0355+54	03:58:53.705(4)	+54:13:13.58(3)	4	03:58:53.708(6)	+54:13:13.80(8)	51499–51966
0452−1759	0450−18	04:52:34.098(3)	−17:59:23.54(7)	4	04:52:34.096(9)	−17:59:23.48(12)	51572–51966
0454+5543	0450+55	04:54:07.621(3)	+55:43:41.2(1)	5	04:54:07.724(7)	+55:43:41.59(9)	51547–51966
0528+2200	0525+21	05:28:52.34(2)	+22:00:00(5)	1	05:28:52.26(3)	+22:00:00.5(70)	51547–51959
0534+2200	0531+21	05:34:31.973(5)	+22:00:52.06(6)	6			51547–51966
0543+2329	0540+23	05:43:09.650(3)	+23:29:06.14(4)	3	05:43:09.67(11)	+23:28:57(49)	51499–51966
0612+3721	0609+37	06:12:48.654(3)	+37:21:37.0(1)	5	06:12:48.653(13)	+37:21:36.6(6)	51607–51938
0630−2834	0628−28	06:30:49.531(6)	−28:34:43.6(1)	1	06:30:49.468(16)	−28:34:42.2(3)	51560–51959
0738−4042	0736−40	07:38:32.432(3)	−40:42:41.15(4)	1	07:38:32.313(4)	−40:42:40.25(6)	51586–51966
0742−2822	0740−28	07:42:49.073(3)	−28:22:44.0(1)	3	07:42:49.030(6)	−28:22:43.25(15)	51560–51966
0814+7429	0809+74	08:14:59.44(4)	+74:29:05.8(1)	2	08:14:59.47(4)	+74:29:05.3(4)	51586–51966
0820−1350	0818−13	08:20:26.358(9)	−13:50:55.20(6)	3	08:20:26.372(7)	−13:50:56.0(3)	51547–51966
0826+2637	0823+26	08:26:51.310(2)	+26:37:25.57(7)	1	08:26:51.500(14)	+26:37:25.5(8)	51547–51967
0837−4135	0835−41	08:37:21.173(6)	−41:35:14.29(7)	7	08:37:21.184(3)	−41:35:14.36(6)	51547–51966
0846−3533	0844−35	08:46:05.9(1)	−35:33:40(2)	8	08:46:05.85(3)	−35:33:39.4(10)	51606–51915
0922+0638	0919+06	09:22:13.977(3)	+06:38:21.69(4)	3	09:22:13.940(17)	+06:38:18.9(8)	51560–51966
0953+0755	0950+08	09:53:09.316(3)	+07:55:35.60(4)	3	09:53:09.23(3)	+07:55:33.2(11)	51547–51966
1136+1551	1133+16	11:36:03.296(4)	+15:51:00.7(1)	9	11:36:03.184(17)	+15:51:10.1(5)	51548–51967
1239+2453	1237+25	12:39:40.475(3)	+24:53:49.25(3)	2	12:39:40.353(12)	+24:53:50.06(18)	51548–51966
1509+5531	1508+55	15:09:25.724(9)	+55:31:33.01(8)	2	15:09:25.666(12)	+55:31:32.55(6)	51548–51966
1645−0317	1642−03	16:45:02.045(3)	−03:17:58.4(1)	1	16:45:02.043(6)	−03:17:58.3(3)	51548–51968
1703−3241	1700−32	17:03:22.4(1)	−32:41:45(4)	2	17:03:22.534(13)	−32:41:48.1(6)	51548–51966
1705−1906	1702−19	17:05:36.108(6)	−19:06:38.5(7)	2	17:05:36.076(8)	−19:06:36.7(14)	51548–51966
1707−4053	1703−40	17:07:21.744(6)	−40:53:55.3(3)	10	17:07:21.728(12)	−40:53:56.1(4)	51573–51925
1709−1640	1706−16	17:09:26.455(2)	−16:40:58.4(3)	1	17:09:26.460(8)	−16:40:58.4(10)	51548–51966
1721−3532	1718−35	17:21:32.80(2)	−35:32:46.6(9)	10	17:21:32.771(11)	−35:32:48.6(4)	51573–51967
1722−3207	1718−32	17:22:02.955(4)	−32:07:44.9(3)	2	17:22:02.951(5)	−32:07:45.6(4)	51506–51967
1740−3015	1737−30	17:40:33.7(1)	−30:15:42(2)	11	17:40:33.753(16)	−30:15:43.8(13)	51549–51967
1741−3927	1737−39	17:41:18.04(3)	−39:27:38(1)	8	17:41:18.071(6)	−39:27:38.41(20)	51549–51967
1745−3040	1742−30	17:45:56.299(2)	−30:40:23.6(3)	2	17:45:56.300(5)	−30:40:23.2(5)	51549–51967
1752−2806	1749−28	17:52:58.66(2)	−28:06:48(5)	1	17:52:58.712(6)	−28:06:35.9(10)	51513–51968
1757−2421	1754−24	17:57:40(60)	−24:21:57(30)	12,13	17:57:29.328(5)		51561–51967
1803−2137	1800−21	18:03:51.35(3)	−21:37:07.2(5)	11	18:03:51.15(4)		51561–51966
1807−0847	1804−08	18:07:38.019(9)	−08:47:43.1(2)	3	18:07:38.036(5)	−08:47:43.3(4)	51500–51966
1818−1422	1815−14	18:18:23.79(5)	−14:22:36(3)	14	18:18:23.770(5)	−14:22:38.9(5)	51549–51960
1820−0427	1818−04	18:20:52.621(3)	−04:27:38.5(1)	1	18:20:52.620(5)	−04:27:37.1(4)	51506–51967
1824−1945	1821−19	18:24:00.45(4)	−19:45:51(8)	8	18:24:00.449(6)	−19:45:49.9(12)	51512–51966
1825−0935	1822−09	18:25:30.596(6)	−09:35:22.8(4)	2	18:25:30.599(7)	−09:35:21.9(6)	51506–51967
1829−1751	1826−17	18:29:43.12(1)	−17:51:03(2)	7	18:29:43.130(10)	−17:50:57.0(9)	51588–51966
1832−0827	1829−08	18:32:37.024(7)	−08:27:03.7(3)	14	18:32:37.017(5)	−08:27:03.0(5)	51500–51967
1833−0827	1830−08	18:33:40.32(2)	−08:27:30.7(6)	14	18:33:40.302(4)	−08:27:31.50(15)	51597–51960
1835−1106		18:35:18.287(2)	−11:06:15.1(2)	15	18:35:18.17(3)	−11:06:19.3(13)	51600–51966
1836−1008	1834−10	18:36:53.9(1)	−10:08:09(5)	16	18:36:53.911(5)	−10:08:09.8(4)	51500–51966
1840+5640	1839+56	18:40:44.59(5)	+56:40:55.6(4)	2	18:40:44.48(4)	+56:40:55.0(4)	51548–51966
1847−0402	1844−04	18:47:22.83(1)	−04:02:14.2(5)	7	18:47:22.833(9)	−04:02:13.8(5)	51550–51966
1848−0123	1845−01	18:48:23.60(2)	−01:23:58.2(7)	7	18:48:23.589(5)	−01:23:57.9(3)	51500–51966

[a] 1. Downs & Reichley, 1983 2. Arzoumanian et al., 1994 3. Fomalont et al., 1992 4. Fomalont et al., 1997 5. Dewey et al., 1988 6. McNamara, 1973, 7. Siegman, Manchester & Durdin, 1993 8. Newton, Manchester & Cooke, 1981 9. Manchester & Taylor, 1981 10. Johnston et al., 1995 11. Braun, Goss and Lyne, 1989 12. Taylor, Manchester and Lyne, 1993 13. Vivekanand, Mohanty & Salter, 1983 14. Clifton et al., 1992 15. Manchester et al., 1996 16. Backus, Taylor & Damashek, 1982 17. Gullahorn & Rankin, 1978 18. Foster, Backer & Wolszczan, 1990

Table 1. *–Continued.*

PSR J	PSR B	α^c(J2000) (^{h} ^{m} ^{s})	δ^c(J2000) ($^\circ$ $'$ $''$)	Ref. [a]	α^o(J2000) (^{h} ^{m} ^{s})	δ^o(J2000) ($^\circ$ $'$ $''$)	Data Span MJD
1900−2600	1857−26	19:00:47.60(1)	−26:00:43.1(3)	3	19:00:47.561(18)	−26:00:39(3)	51573–51967
1913−0440	1911−04	19:13:54.18(1)	−04:40:47.6(4)	9	19:13:54.184(5)	−04:40:47.6(3)	51550–51966
1917+1353	1915+13	19:17:39.784(2)	+13:53:57.06(9)	2	19:17:39.790(4)	+13:53:56.80(9)	51573–51966
1921+2153	1919+21	19:21:44.798(3)	+21:53:01.83(8)	9	19:21:44.80(3)	+21:53:02.8(5)	51600–51966
1932+1059	1929+10	19:32:13.900(2)	+10:59:31.99(7)	2	19:32:13.9430(15)	+10:59:32.52(6)	51550–51960
1935+1616	1933+16	19:35:47.835(1)	+16:16:40.59(2)	1	19:35:47.8249(11)	+16:16:40.03(4)	51550–51966
1946+1805	1944+17	19:46:53.043(4)	+18:05:41.59(9)	17	19:46:53.05(3)	+18:05:41.5(8)	51560–51966
1948+3540	1946+35	19:48:25.037(2)	+35:40:11.28(2)	17	19:48:25.006(3)	+35:40:11.03(6)	51500–51966
1955+5059	1953+50	19:55:18.90(6)	+50:59:54.2(6)	16	19:55:18.736(6)	+50:59:55.76(10)	51513–51966
2002+4050	2000+40	20:02:44.04(3)	+40:50:54.7(3)	5	20:02:44.047(10)	+40:50:53.99(19)	51560–51966
2013+3845	2011+38	20:13:10.49(3)	+38:45:44.8(3)	5	20:13:10.384(7)	+38:45:43.08(16)	51549–51966
2018+2839	2016+28	20:18:03.851(2)	+28:39:54.26(3)	1	20:18:03.832(4)	+28:39:54.26(9)	51549–51966
2022+2854	2020+28	20:22:37.079(3)	+28:54:23.45(3)	18	20:22:37.078(3)	+28:54:22.91(6)	51547–51967
2022+5154	2021+51	20:22:49.900(2)	+51:54:50.06(2)	1	20:22:49.843(10)	+51:54:50.46(16)	51547–51968
2048−1616	2045−16	20:48:35.472(4)	−16:16:44.45(8)	3	20:48:35.46(8)	−16:16:38(4)	51547–51960
2108+4441	2106+44	21:08:20.48(1)	+44:41:48.8(1)	2	21:08:20.521(8)	+44:41:49.37(16)	51547–51966
2113+4644	2111+46	21:13:24.29(1)	+46:44:08.7(1)	2	21:13:24.377(10)	+46:44:09.1(3)	51547–51966
2157+4017	2154+40	21:57:01.82(1)	+40:17:45.9(1)	2	21:57:01.879(13)	+40:17:45.8(4)	51547–51966
2219+4754	2217+47	22:19:48.136(4)	+47:54:53.83(4)	2	22:19:48.115(10)	+47:54:53.73(12)	51506–51966
2257+5909	2255+58	22:57:57.711(4)	+59:09:14.95(3)	2	22:57:57.756(9)	+59:09:14.93(9)	51547–51966
2313+4253	2310+42	23:13:08.571(6)	+42:53:12.98(3)	3	23:13:08.622(10)	+42:53:13.12(19)	51547–51967
2321+6024	2319+60	23:21:55.19(4)	+60:24:30.7(3)	2	23:21:55.16(3)	+60:24:30.58(16)	51499–51966
2326+6113	2324+60	23:26:58.704(5)	+61:13:36.50(3)	2	23:26:58.693(8)	+61:13:36.29(8)	51560–51966
2354+6155	2351+61	23:54:04.71(2)	+61:55:46.8(1)	2	23:54:04.743(16)	+61:55:46.67(12)	51547–51966

[a] 1. Downs & Reichley, 1983 2. Arzoumanian et al., 1994 3. Fomalont et al., 1992 4. Fomalont et al., 1997 5. Dewey et al., 1988 6. McNamara, 1973, 7. Siegman, Manchester & Durdin, 1993 8. Newton, Manchester & Cooke, 1981 9. Manchester & Taylor, 1981 10. Johnston et al., 1995 11. Braun, Goss and Lyne, 1989 12. Taylor, Manchester and Lyne, 1993 13. Vivekanand, Mohanty & Salter, 1983 14. Clifton et al., 1992 15. Manchester et al., 1996 16. Backus, Taylor & Damashek, 1982 17. Gullahorn & Rankin, 1978 18. Foster, Backer & Wolszczan, 1990

10^{-8} s less than predicted. The observed period change in PSR B1737−30 is huge, with $\Delta P \sim 1.2 \times 10^{-6}$ s, much larger than for other pulsars. This pulsar glitched frequently during MJD 46301–49400, with nine glitches being detected (Shemar & Lyne 1996), i.e., on average, one glitch every 11 months. It has been more than six years since Shemar & Lyne's work until our observations started, so it is probable that there were several glitches during this interval.

Fig. 5 shows a histogram of the observed period changes excepting PSR B1737−30 and the Crab pulsar. Also, pulsars are not included if the uncertainties in ΔP or $\Delta\dot{P}$ are larger than 20 ns or 30×10^{-18} respectively, eliminating PSRs B0525+21, B0844−35, B1700−32, B1754−24 and B1800−21. With these exceptions, most period changes are small, with $|\Delta P| \lesssim 3$ ns.

We find an interesting correlation between ΔP and $\Delta\dot{P}$, illustrated in Fig. 6. This plot shows a strong tendency for ΔP and $\Delta\dot{P}$ to have the same sign and to be correlated in amplitude. For random period noise we would expect these two quantities to be uncorrelated. However, glitches involve systematic changes in both P and $\dot{P}$ and we investigate this further.

In most cases, the pulse frequency after a glitch is well modelled by the relation

$$\nu(t) = \nu_0(t) + \Delta\nu_g[1 - Q(1 - \exp(-t/\tau_d)] + \Delta\dot{\nu}_p t, \qquad (3)$$

where $\nu_0(t)$ is the value of ν extrapolated from before the glitch, $\Delta\nu_g$ is the total frequency change at the time of the glitch, Q is the fractional part of $\Delta\nu_g$ which decays exponentially, τ_d is the decay time constant and $\Delta\dot{\nu}_p$ is the permanent change in $\dot{\nu}$ at the time of the glitch (Wang et al. 2000). The increment in frequency derivative is given by:

$$\Delta\dot{\nu}(t) = \frac{-Q\Delta\nu_g}{\tau_d} \exp(-t/\tau_d) + \Delta\dot{\nu}_p. \qquad (4)$$

We use these relations to compute P and $\dot{P}$ at an arbitrary time t in the *past*, and compare them with the values at the *current* time t_0, assuming a glitch of magnitude $\Delta\nu_g = 10^{-6}$ at time $t_0 - t = 400$ days. Values of $\Delta P = P_0 - P$ and $\Delta\dot{P} = \dot{P}_0 - \dot{P}$ are shown as a function of $t_0 - t$ in Fig. 7. If a pulsar glitched before the previous observation, both ΔP and $\Delta\dot{P}$ will be negative; while if the glitch happened between the observations, we have $\Delta P < 0$ and $\Delta\dot{P} < 0$ for negative $\Delta\dot{P}_{\rm p} = -\Delta\dot{\nu}_{\rm p}/\nu^2$, and $\Delta P > 0$ and $\Delta\dot{P} > 0$ for positive $\Delta\dot{P}_{\rm p}$ and large fractional decay Q. These predictions are consistent with the observations shown in Fig. 6. The last case represents the observed situation in the Crab pulsar (Lyne, Pritchard & Smith 1993). For positive $\Delta P_{\rm p}$ and small Q, we can have $\Delta P < 0$ and $\Delta\dot{P} > 0$. Furthermore, in this model there is no case with $\Delta P > 0$ and $\Delta\dot{P} < 0$, consistent with the observed deficit in the lower-right of Fig. 6. For $Q > 0$ in a glitch before the first observation, the changes in

Table 2. Pulsar period parameters at MJD 51700.

PSR J	PSR B	P (s)	$\dot{P}$ (10^{-15})	$N_{\rm toa}$	Res. (μs)	ΔP (10^{-9} s)	$\Delta\dot{P}$ (10^{-18})	ΔT (yr)	Ref.[a]
0034−0721	0031−07	0.94295117325(7)	0.395(13)	25	854	−0.03(87)	−13(13)	30.1	1
0139+5814	0136+57	0.272452862190(3)	10.7040(6)	60	268	3.07(9)	3.4(6)	9.1	2
0141+6009	0138+59	1.22294860175(7)	0.417(17)	41	756	0.4(7)	26(17)	27.1	3
0332+5434	0329+54	0.714520624711(5)	2.0489(10)	102	469	−1.19(8)	−0.7(10)	30.3	1
0358+5413	0355+54	0.1563832093117(10)	4.3954(3)	61	342	0.66(10)	5.0(5)	14.2	4
0452−1759	0450−18	0.548940421758(19)	5.753(3)	54	546	−1.31(18)	−4(3)	13.4	5
0454+5543	0450+55	0.340729803314(5)	2.3742(8)	59	321	1.95(6)	8.6(8)	9.0	2
0528+2200	0525+21	3.74553060709(15)	40.01(3)	52	893	2(11)	−16(36)	26.4	4
0543+2329	0540+23	0.245978510226(3)	15.4205(7)	65	568	−0.764(18)	−3.8(7)	9.1	2
0612+3721	0609+37	0.297982336991(18)	0.059(3)	21	293	0.23(6)	0.05(300)	15.3	6
0630−2834	0628−28	1.24442173630(8)	7.195(14)	53	1171	11(6)	88(16)	20.7	7
0738−4042	0736−40	0.374919985032(6)	1.6161(9)	44	171	−1.3(3)	2.0(9)	25.0	7
0742−2822	0740−28	0.166765742577(5)	16.8177(8)	62	575	3.20(6)	5.2(8)	9.1	2
0814+7429	0809+74	1.29224148381(11)	0.153(16)	57	1119	0.03(26)	−15(16)	9.1	2
0820−1350	0818−13	1.23813005246(4)	2.097(6)	58	644	−0.24(19)	−8(6)	29.3	1
0826+2637	0823+26	0.530661285865(12)	1.6978(19)	66	588	−1.61(12)	−11.6(20)	9.1	2
0837−4135	0835−41	0.751623617646(8)	3.5393(12)	33	165	−1.8(3)	−7.6(13)	13.4	5
0846−3533	0844−35	1.1160975763(3)	1.62(5)	30	1046	22(22)	48(53)	22.3	8
0922+0638	0919+06	0.430623569113(12)	13.6924(19)	54	521	−1.18(15)	−28.1(20)	9.0	2
0953+0755	0950+08	0.253065270746(6)	0.2288(10)	69	540	0.62(10)	−0.4(10)	27.9	9
1136+1551	1133+16	1.18791477322(3)	3.733(5)	73	661	0.60(7)	0.6(48)	27.5	9
1239+2453	1237+25	1.38244953180(4)	0.967(7)	67	677	−0.15(15)	6(7)	9.1	2
1509+5531	1508+55	0.739682698169(16)	4.996(3)	58	512	−2.68(9)	−12(3)	9.1	2
1645−0317	1642−03	0.387690495052(10)	1.7924(15)	67	595	−1.04(10)	11.4(15)	30.3	1
1703−3241	1700−32	1.21178519124(4)	0.660(7)	57	709	−36(31)	−130(97)	10.1	2
1705−1906	1702−19	0.298988488005(8)	4.1370(14)	55	603	−0.244(20)	−1.3(14)	9.2	2
1707−4053	1703−40	0.581016707860(18)	1.925(4)	23	280	0.19(7)	5(4)	9.1	2
1709−1640	1706−16	0.65305652375(3)	6.240(4)	50	675	−11.99(12)	−69(4)	9.1	2
1721−3532	1718−35	0.280424567967(9)	25.1816(14)	52	497	−4.28(9)	−14.5(15)	9.1	2
1722−3207	1718−32	0.477157619208(5)	0.6475(9)	57	378	−0.25(4)	0.4(9)	9.1	2
1740−3015	1737−30	0.60676381008(3)	466.312(5)	48	893	−1181(9)	291(54)	6.7	4
1741−3927	1737−39	0.512211401067(8)	1.9313(14)	44	319	68(3)	122(5)	22.3	8
1745−3040	1742−30	0.367430422265(6)	10.6696(10)	54	327	0.86(3)	4.5(10)	9.1	2
1752−2806	1749−28	0.562561300009(9)	8.1271(16)	62	550	2.0(7)	5(3)	9.5	5
1757−2421	1754−24	0.234102570587(4)	12.9146(5)	51	373	−54(192)	−100(300)	20.2	10
1803−2137	1800−21	0.133641979388(15)	134.150(3)	36	2378	5(6)	206(200)	1.9	11
1807−0847	1804−08	0.163727380271(3)	0.0287(5)	58	725	0.09(7)	0.03(48)	21.4	3
1818−1422	1815−14	0.291489038008(5)	2.0399(9)	49	316	0.9(3)	3.0(11)	12.9	12
1820−0427	1818−04	0.598078699467(10)	6.3379(20)	60	744	−6.1(5)	0.2(21)	30.3	1
1824−1945	1821−19	0.189335814049(3)	5.2394(5)	63	519	2.3(6)	14.5(14)	13.4	5
1825−0935	1822−09	0.768994380569(16)	52.336(4)	59	909	−33.5(3)	−29(4)	9.1	2
1829−1751	1826−17	0.307133849665(11)	5.5414(16)	50	420	−4.17(13)	−20.6(16)	13.4	5
1832−0827	1829−08	0.647305181037(9)	63.8874(20)	55	713	−3.70(17)	−5.8(20)	12.9	12
1833−0827	1830−08	0.0852852156141(15)	9.1721(3)	39	145	0.30(5)	2.6(3)	10.0	4
1835−1106		0.165910996503(20)	20.656(3)	27	915	3.896(20)	44(3)	6.2	13
1836−1008	1834−10	0.562713612837(7)	11.8013(14)	58	618	15(5)	26(7)	21.4	3
1840+5640	1839+56	1.65286223816(14)	1.51(3)	46	1812	−0.01(88)	10(24)	9.1	2
1847−0402	1844−04	0.59778239230(3)	51.704(4)	50	708	−2.3(5)	−10(4)	13.4	5
1848−0123	1845−01	0.659432812074(9)	5.2479(18)	58	709	11.6(7)	29(3)	13.4	5
1900−2600	1857−26	0.61220925419(4)	0.193(6)	49	788	0.20(6)	−11(6)	9.1	2

[a] 1. Manchester & Taylor, 1981 2. Arzoumanian et al., 1994 3. Backus, Taylor & Damashek, 1982 4. Shemar & Lyne, 1996 5. Siegman, Manchester & Durdin, 1993 6. Dewey et al., 1988 7. Manchester et al. 1983 8. Newton, Manchester & Cooke, 1981 9. Gullahorn & Rankin, 1978 10. Vivekanand, Mohanty & Salter, 1983 11. Wang et al., 2000 12. Clifton et al., 1992 13. Manchester et al., 1996 14. Foster, Backer & Wolszczan, 1990

Table 2. Pulsar period parameters at MJD 51700.

PSR J	PSR B	P (s)	$\dot{P}$ (10^{-15})	$N_{\rm toa}$	Res. (μs)	ΔP (10^{-9} s)	$\Delta\dot{P}$ (10^{-18})	ΔT (yr)	Ref.[a]
1913−0440	1911−04	0.825937582927(13)	4.055(3)	47	301	−1.37(20)	−14(3)	30.3	1
1917+1353	1915+13	0.1946321872566(13)	7.19502(18)	49	256	−0.150(18)	−3.22(19)	9.1	2
1921+2153	1919+21	1.33730247470(8)	1.358(8)	26	1151	−0.02(9)	10(8)	30.1	1
1932+1059	1929+10	0.2265181529285(15)	1.1618(3)	39	120	0.39(4)	5.2(3)	9.1	2
1935+1616	1933+16	0.3587411416716(16)	6.0023(3)	42	84	−0.91(5)	−1.4(3)	25.8	9
1946+1805	1944+17	0.44061848299(3)	0.020(3)	54	2234	−0.07(7)	−4(3)	9.1	2
1948+3540	1946+35	0.717312547254(5)	7.0592(10)	54	340	6.06(8)	7.0(10)	26.0	9
1955+5059	1953+50	0.518938338380(8)	1.3722(15)	59	539	4.0(14)	6(3)	21.4	3
2002+4050	2000+40	0.90506709268(4)	1.743(6)	53	757	−2.6(10)	−0.9(62)	15.3	6
2013+3845	2011+38	0.230195129550(7)	8.8514(11)	50	602	−1.52(20)	−3.7(12)	15.4	6
2018+2839	2016+28	0.557953548298(8)	0.1478(13)	42	282	−1.08(3)	−1.6(13)	30.1	1
2022+2854	2020+28	0.343402486392(4)	1.8924(6)	44	203	0.3(3)	−1.1(8)	12.8	14
2022+5154	2021+51	0.529198257306(18)	3.061(3)	72	884	−0.73(4)	−4(3)	9.1	2
2048−1616	2045−16	1.96157730029(5)	10.973(9)	41	474	−2.15(20)	12(9)	30.1	1
2108+4441	2106+44	0.414870558915(12)	0.095(3)	52	679	−0.02(5)	9(3)	9.1	2
2113+4644	2111+46	1.01468510534(4)	0.719(7)	48	834	−0.84(18)	7(7)	9.1	2
2157+4017	2154+40	1.52526635476(9)	3.434(14)	61	1308	4.0(3)	8(14)	9.1	2
2219+4754	2217+47	0.538470040747(10)	2.7634(20)	57	800	0.13(3)	−1.6(20)	9.1	2
2257+5909	2255+58	0.368247257217(8)	5.7555(13)	61	490	−0.19(5)	1.7(13)	9.0	2
2313+4253	2310+42	0.349433715696(12)	0.111(3)	58	819	−2.0(6)	−4(3)	21.4	3
2321+6024	2319+60	2.25648988440(7)	7.017(13)	58	1322	0.3(6)	−20(13)	9.1	2
2326+6113	2324+60	0.233652031097(5)	0.3513(8)	53	360	−0.008(10)	−1.3(8)	9.0	2
2354+6155	2351+61	0.94478711093(3)	16.248(5)	56	685	−0.59(12)	−16(5)	9.1	2

[a] 1. Manchester & Taylor, 1981 2. Arzoumanian et al., 1994 3. Backus, Taylor & Damashek, 1982 4. Shemar & Lyne, 1996 5. Siegman, Manchester & Durdin, 1993 6. Dewey et al., 1988 7. Manchester et al. 1983 8. Newton, Manchester & Cooke, 1981 9. Gullahorn & Rankin, 1978 10. Vivekanand, Mohanty & Salter, 1983 11. Wang et al., 2000 12. Clifton et al., 1992 13. Manchester et al., 1996 14. Foster, Backer & Wolszczan, 1990

Table 3. Pre-glitch ephemeris of the Crab pulsar.

PSR	B0531+21 (J0534+2200)
RAJ	$05^{\rm h}34^{\rm m}31\overset{\rm s}{.}972$
DECJ	$22^\circ00'52\overset{''}{.}07$
PEPOCH	51562.7279
ν (s^{-1})	29.845547780
$\dot{\nu}$ (s^{-2})	-3.7457341×10^{-10}
$\ddot{\nu}$ (s^{-3})	1.0161006×10^{-20}
$\dddot{\nu}$ (s^{-4})	-6.0×10^{-31}
DM (cm^{-3} pc)	56.77

ΔP and $\Delta\dot{P}$ are proportional, also consistent with the observations shown in Fig. 6. These agreements strongly suggest that long-term systematic changes in pulsar periods and their derivatives are dominated by pulsar glitches (cf. Lyne 1996; Johnston & Galloway 1999).

4.3 The Crab Pulsar

Observations of the Crab pulsar revealed a glitch during 2000 July. This glitch was also observed at Jodrell Bank Observatory and the pre-glitch ephemeris given in Table 3 is based on Jodrell Bank data. They also determined the glitch epoch to be MJD 51740.8 (2000 July 15). We use these parameters in our analyses.

Table 4. Rotation parameters after the 2000 July glitch.

Epoch (MJD)	51856.0000
Data span	51745.2–51966.6
ν (s^{-1})	29.836059670(2)
$\dot{\nu}$ (s^{-2})	$-3.743460(3)\times10^{-10}$
$\ddot{\nu}$ (s^{-3})	$1.17(2)\times10^{-20}$

Residuals relative to the model in Table 3 are shown in Fig. 8 and Fig. 9 shows the observed variations in frequency and frequency derivative. We estimate the time constant of the glitch, τ_d, to be 4 days. This value gives phase continuity at the adopted glitch epoch and we keep it fixed during the analyses. Fitting of the glitch model described in Equation 3 using TEMPO gives a glitch size $\Delta\nu/\nu \sim 24(8)\times10^{-9}$, an increment in $\Delta\dot{\nu}/\dot{\nu} \sim 5(2)\times10^{-3}$, and $Q = 0.8$, that is 80 per cent of the jump in frequency decays away on the given timescale τ_d. As may be seen in Fig. 9, there is a persistent increase in the magnitude of the slow-down rate; fitting for this in TEMPO gives $\Delta\dot{\nu}_p \sim -48(3)\times10^{-15}$ s^{-2}. Rotation parameters for the post-glitch data obtained using TEMPO are given in Table 4.

Glitches in the Crab pulsar are frequent and have relative sizes in the range 4.7×10^{-9} to 85×10^{-9} (Lyne, Pritchard & Smith 1993; Wong, Backer & Lyne 2001). Lyne et al. (1993) showed that two of the largest Crab glitches

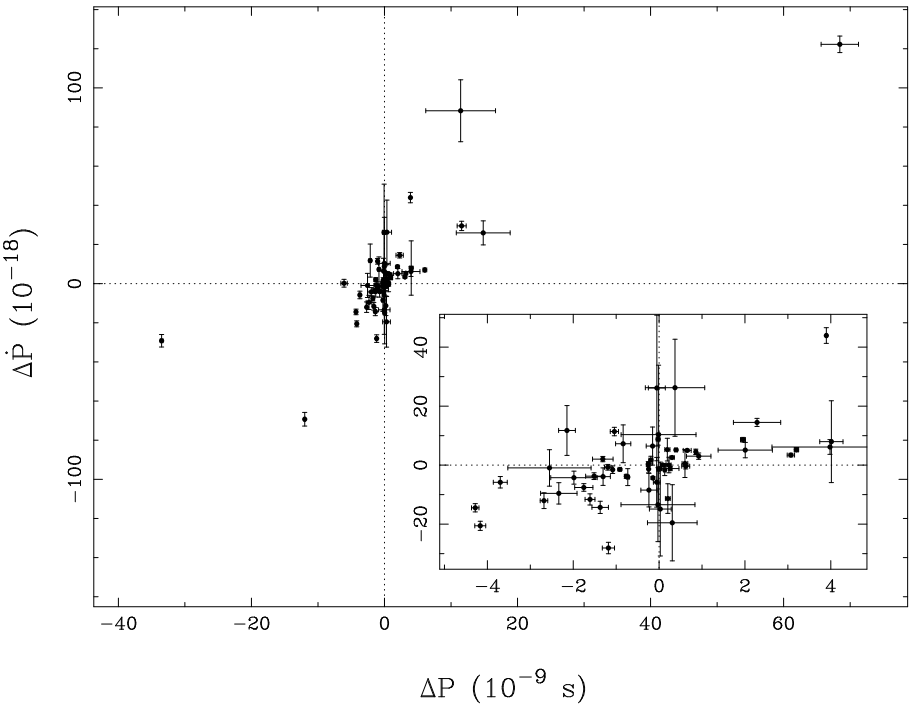

Figure 6. Difference between observed and predicted period derivative $\Delta\dot{P}$, plotted against difference in period, ΔP. The inset is an expanded version of the central region. The data set is the same as in Fig. 5.

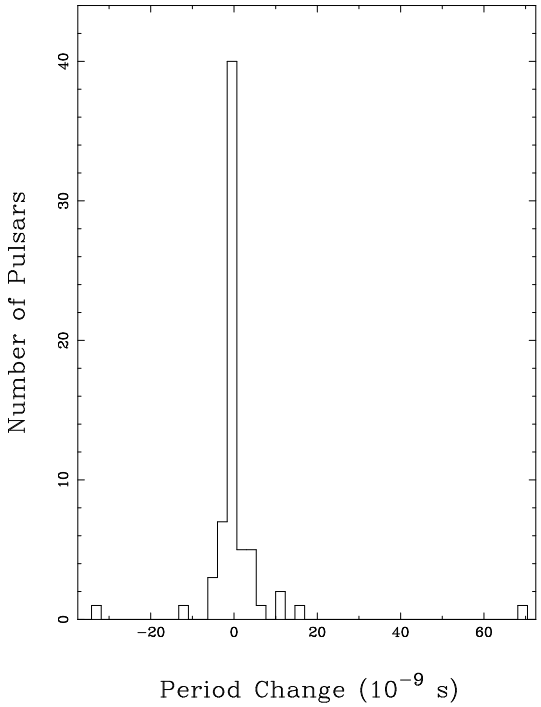

Figure 5. Histogram of pulsar period changes. The Crab pulsar and PSR B1737−30 are not included as they suffered glitches, five other pulsars with large uncertainties in ΔP and $\Delta\dot{P}$ are excluded as well.

($\Delta\nu/\nu \sim 37$ and 85×10^{-9}) had persistent increases in slowdown rate, so that the Crab pulsar is now rotating more slowly than it would have without the glitches. It is clear that the 2000 July glitch falls into the class of large glitches in the Crab pulsar.

5 DISCUSSION

We have developed a pulsar timing system for the 25-m Nanshan radio telescope of Urumqi Astronomical Observatory and used it to determine positions and period parameters for 74 pulsars. Typical timing residuals over one year are few hundred microseconds, giving positions typically to a few tenths of an arcsec and pulse periods to 0.01 ns or better. Comparison with earlier measurements has shown that long-term period fluctuations are probably dominated by recovery from (mostly unseen) glitches.

A cryogenic receiver system operating in the 18-cm band for the UAO Nanshan telescope is currently under construction. This will enable timing and other measurements to be made on pulsars with mean flux density as low as 1 mJy. Compared to larger radio telescopes, frequent pulsar observations are possible with this system, making it ideal for projects such as the study of pulsar timing irregularities and scintillation. The higher sensitivity of the cryogenic system will allow more precise timing and observations of a larger sample of pulsars.

ACKNOWLEDGEMENTS

We thank the engineers responsible for maintaining the receiver, telescope and H-maser at UAO, and the staff who helped with the observations. The filterbank/digitiser system was designed and constructed at Jodrell Bank Observatory, University of Manchester, and the downconvertor sys-

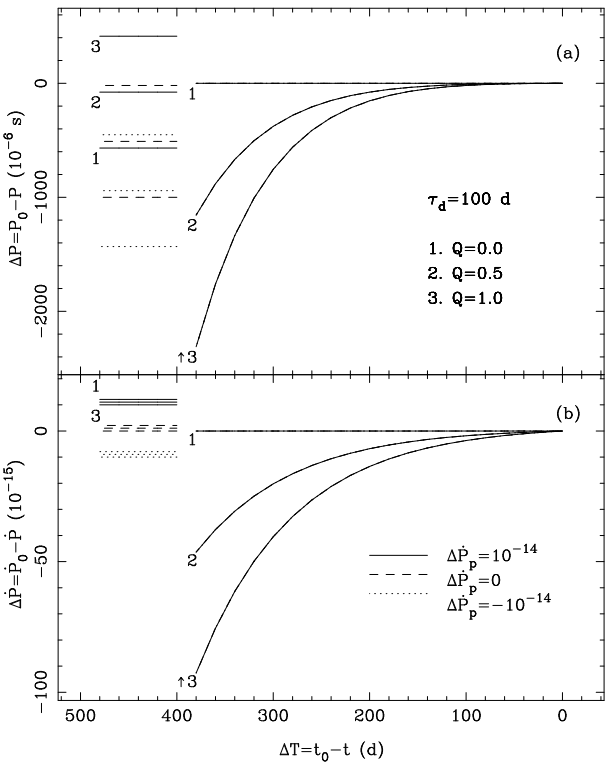

Figure 7. A model for the increments in pulse period and period derivative due to a glitch occurring 400 days before the current time t_0. A glitch magnitude $\Delta\nu_g = 10^{-6}$ and a post-glitch decay time of 100 days are assumed. Changes for three different decay parameters Q and three different permanent changes in period derivative $\Delta\dot{P}_p$ are plotted. The groups of three lines of one type are for different values of Q and the solid, dashed and dotted lines represent different values of $\Delta\dot{P}_p$. The post-glitch values are functions of Q and independent of $\Delta\dot{P}_p$, so they overlap for different $\Delta\dot{P}_p$.

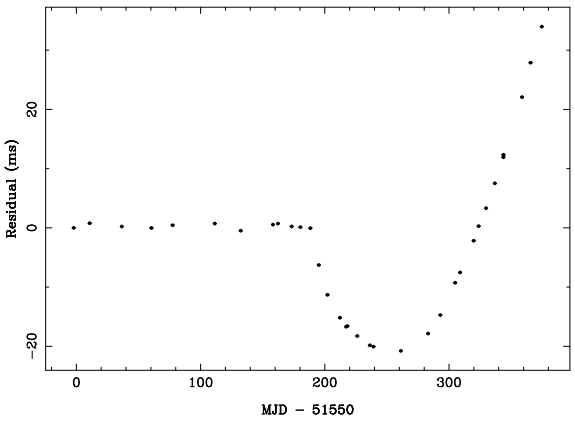

Figure 8. Timing residual of the Crab pulsar showing the glitch of 2000 July.

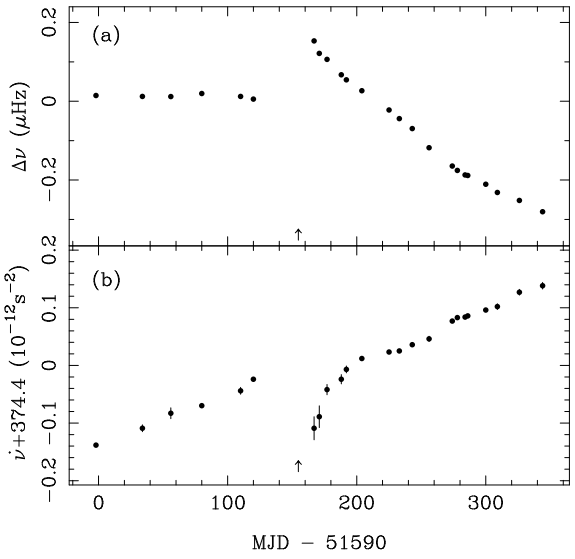

Figure 9. A glitch of the Crab pulsar at epoch MJD 51741. (a) frequency residual $\Delta\nu$ relative to the pre-glitch solution and (b) the variation of $\dot{\nu}$. The glitch epoch is indicated by an arrow near the bottom of each plot.

tem was built at the Australia Telescope National Facility. We thank them for their support. NW thanks Beijing Astrophysics Center for providing computer facilities, the ATNF for a Postgraduate Research Scholarship and the National Nature Science Foundation of China for supporting the timing project.

REFERENCES

Arzoumanian Z., Nice D. J., Taylor J. H., Thorsett S. E., 1994, ApJ, 422, 671
Backus P. R., Taylor J. H., Damashek M., 1982, ApJ, 255, L63
Braun R., Goss W. M., Lyne A. G., 1989, ApJ, 340, 355
Clifton T. R., Lyne A. G., Jones A. W., McKenna J., Ashworth M., 1992, MNRAS, 254, 177
Cordes J. M., Downs G. S., 1985, ApJS, 59, 343
Dewey R. J., Taylor J. H., Weisberg J. M., Stokes G. H., 1985, ApJ, 294, L25
Dewey R. J., Taylor J. H., Maguire C. M., Stokes G. H., 1988, ApJ, 332, 762
Downs G. S., Reichley P. E., 1983, ApJS, 53, 169
Fomalont E. B., Goss W. M., Lyne A. G., Manchester R. N., Justtanont K., 1992, MNRAS, 258, 497
Fomalont E. B., Goss W. M., Manchester R. N., Lyne A. G., 1997, MNRAS, 286, 81
Foster R. S., Backer D. C., Wolszczan A., 1990, ApJ, 356, 243
Gullahorn G. E., Rankin J. M., 1978, AJ, 83, 1219
Johnston S., Galloway D., 1999, MNRAS, 306, L50
Johnston S., Manchester R. N., Lyne A. G., Kaspi V. M., D'Amico N., 1995, A&A, 293, 795
Lyne A. G., 1996, in Johnston S., Walker M. A., Bailes M., eds, Pulsars: Problems and Progress, IAU Colloquium 160. Astronomical Society of the Pacific, San Francisco, p. 73
Lyne A. G., Pritchard R. S., Smith F. G., 1993, MNRAS, 265, 1003
Lyne A. G., Shemar S. L., Graham-Smith F., 2000, MNRAS, 315, 534
Manchester R. N., Taylor J. H., 1981, AJ, 86, 1953
Manchester R. N., Newton L. M., Hamilton P. A., Goss W. M., 1983, MNRAS, 202, 269
Manchester R. N. et al., 1996, MNRAS, 279, 1235
McNamara B. J., 1971, PASP, 83, 491
Newton L. M., Manchester R. N., Cooke D. J., 1981, MNRAS,

194, 841
Shemar S. L., Lyne A. G., 1996, MNRAS, 282, 677
Siegman B. C., Manchester R. N., Durdin J. M., 1993, MNRAS, 262, 449
Standish E. M., 1982, A&A, 114, 297
Taylor J. H., Manchester R. N., Lyne A. G., 1993, ApJS, 88, 529
Vivekanand M., Mohanty D. K., Salter C. J., 1983, MNRAS, 204, 81P
Wang N., Manchester R. N., Pace R., Bailes M., Kaspi V. M., Stappers B. W., Lyne A. G., 2000, MNRAS, 317, 843
Wong T., Backer D. C., Lyne A., 2001, ApJ, 548, 447